

Volovik effect on NMR measurements of unconventional superconductors

Yunkyu Bang*

Department of Physics, Chonnam National University, Kwangju 500-757, Republic of Korea

(Dated: August 15, 2018)

We studied the Volovik effect on the NMR measurements of the two unconventional superconducting (SC) states, the d-wave and $\pm s$ -wave states. We showed the generic field dependencies of the spin-lattice relaxation rate $1/T_1$ and Knight shift K at low temperature limit in the pure cases as: $1/T_1 \propto H \log H$, $K \propto \sqrt{H}$ for the d-wave, and $1/T_1 \propto H$, $K \propto H$ for the $\pm s$ -wave state, respectively. Performing numerical calculations we showed that these generic power laws survive for the good part of low field region with the realistic amount of impurities. We also found that the Volovik effect acts as an equivalent pair breaker as the unitary impurity scattering, hence induces the same temperature evolutions on $1/T_1$ and K , respectively, as the unitary impurities in both SC states. This finding implies that the Volovik effect should always be taken into account for the analysis of the NMR measurements in the mixed state.

PACS numbers: 74.20.Rp, 74.25.fc, 74.25.Uv

Introduction. – There are various experimental probes of the gap symmetry of the superconductors. Mostly, they are probing low lying excitations in the superconducting (SC) state to distinguish a full gap, a nodal, or a point gap. The measurement results usually produce the typical temperature dependencies, for example, an exponentially flat for a full gap or various power laws for a nodal or point gap. The Volovik effect (VE) [1] has enlarged the probing dimension to the magnetic field axis. The principle is actually very simple in that the low energy density of states (DOS) of the SC state is changed in the mixed state with vortices induced by the applied magnetic fields and then its field dependence is probed. In particular, this change of DOS due to the vortices should be more sensitive with a gapless superconductor such as the d-wave state in the cuprate superconductors [1, 2]. However, recently, it was shown that the strong field dependence of the Volovik effect is not unique to the nodal gap superconductors but also can appear with the full gap s-wave superconductors if there exist multiple s-wave gaps with different gap sizes [3].

On the other hand, most of the Volovik effect measurements have been carried out with the specific heat (SH) and thermal conductivity. However, in principle, it should be effective with any experimental measurements which probe the low energy DOS and its variation with the applied field. Therefore, the NMR measurements such as the spin-lattice relaxation rate $1/T_1(T, H)$ and Knight shift $K(T, H)$ should also be good probes for the Volovik effect. In comparison with the SH and thermal conductivity measurements, the NMR measurements of Volovik effect require much harsher conditions such as the sample size, low temperature control, and high quality homogeneity of the field, etc. Nevertheless there already exist a few experimental works, for example, on Fe pnictide superconductors, $\text{Ba}_{0.69}\text{K}_{0.31}\text{Fe}_2\text{As}_2$ by W. P. Halperin and coworkers[4] and $\text{BaFe}_2\text{As}_2(\text{As}_{0.67}\text{P}_{0.33})_2$ by Nakai *et al.*[5], as well as on the high- T_c cuprates by G. Q. Zheng and coworkers [6]. However, because the theoretical study on this subject is very rare [7], the reliable interpretation and the extraction of the useful information from the experimental data are limited. Therefore more systematic and detailed theoret-

ical study of the Volovik effects on the NMR measurements is highly demanded and it will enhance the capability of the NMR technique to study the superconducting gap symmetry.

In this paper, we specifically studied the NMR $1/T_1$ and Knight shift K in the SC state of the two typical unconventional superconductors, namely, the d-wave and $\pm s$ -wave states[8, 9]. We derived the exact power laws of the generic field dependencies of both SC cases in pure state: $1/T_1 \propto H \log H$, $K \propto \sqrt{H}$ for the d-wave, and $1/T_1 \propto H$, $K \propto H$ for the $\pm s$ -wave state, respectively. We also numerically studied the impurity effects on $1/T_1$ and K , using the self-consistent T -matrix approximation (SCTA) [10, 11], and provided the systematic comparison between the d-wave and $\pm s$ -wave gap states. We found that the impurity scattering substantially reduces the low field region where the generic field dependencies survive in the $\pm s$ -wave case, while it doesn't much affect the generic power laws except a constant shifting in the d-wave case [12]. Another key finding of our numerical study is that the Volovik effect induced by magnetic fields practically acts as an equivalent pair breaker as the strong coupling (unitary limit) impurities, hence modifies the low temperature behaviors of the $1/T_1$ and K in the same fashion as due to the formation of the resonant impurity band. This result implies that it is always necessary to take the Volovik effect into account when one interprets the low temperature NMR experiments with magnetic field in order to extract the correct information from the data.

Formalism. – For most of purposes to study the Volovik effect, we just need to calculate the position dependent DOS $N(\omega, r)$ in the presence of vortices. Using the semiclassical approximation, the matrix form of the single-particle Green's function in the SC state, including Doppler shift of the quasi-particle excitations $\epsilon(k)$ due to the circulating supercurrent $\mathbf{v}_s(\mathbf{r})$, is given by [1, 2]

$$\hat{G}(\mathbf{k}, \mathbf{r}, \omega) = \frac{[\omega + \mathbf{v}_s(\mathbf{r}) \cdot \mathbf{k}] \tau_0 + \epsilon(k) \tau_3 + \Delta \tau_1}{[\omega + \mathbf{v}_s(\mathbf{r}) \cdot \mathbf{k}]^2 - \epsilon^2(k) - \Delta^2} \quad (1)$$

where τ_i are Pauli matrices and \mathbf{r} is the distance from the vortex core. Δ is the SC gap function and $\mathbf{v}_s(\mathbf{r})$ is $\sim \frac{1}{m} \frac{\hat{\theta}}{r}$.

The position dependent DOS is calculated as $N(\omega, r) = -\frac{1}{\pi} \text{TrIm} \sum_k G_0(\mathbf{k}, \mathbf{r}, \omega)$. Finally, the field dependent quantities are obtained from the areal average DOS per unit volume as $\bar{N}(\omega, H) = \int_{\xi}^{R_H} dr^2 N(\omega, r) / \pi R_H^2$ with the magnetic length $R_H = \sqrt{\frac{\Phi_0}{\pi H}}$ (Φ_0 a flux quanta) and the SC coherence length ξ .

In the homogeneous SC state, the general structure of the $1/T_1$ is written as

$$\frac{1}{T_1} = -T \int_0^{\infty} d\omega \frac{\partial f_{FD}(\omega)}{\partial \omega} [N(\omega)^2 + M(\omega)^2], \quad (2)$$

and the Knight shift K as

$$K = -T \int_0^{\infty} d\omega \frac{\partial f_{FD}(\omega)}{\partial \omega} N(\omega), \quad (3)$$

where $N(\omega) = \langle \text{Re} \frac{\omega}{\sqrt{\omega^2 - \Delta^2(\theta)}} \rangle_{\theta}$ is the Fermi surface (FS) averaged DOS and $M(\omega) = \langle \text{Re} \frac{\Delta(\theta)}{\sqrt{\omega^2 - \Delta^2(\theta)}} \rangle_{\theta}$ is the similar quantity induced in the SC state. In the mixed state, we only need to replace $N(\omega)$ by $\bar{N}(\omega, H)$ and $M(\omega)$ by $\bar{M}(\omega, H)$ in the above formulas (2) and (3). $\bar{M}(\omega, H)$ is obtained from $M(\omega, r) = -\frac{1}{\pi} \text{TrIm} \sum_k G_1(\mathbf{k}, \mathbf{r}, \omega)$ and its areal average. Then we can calculate the field as well as temperature dependent NMR properties $1/T_1(T, H)$ and $K(T, H)$.

In the mixed state of the d-wave superconductor, it is well known that the $N(\omega = 0, r) \sim 1/r$ due to the linear DOS $N(\omega) \sim \omega$ and the Doppler shifting energy $\mathbf{v}_s(\mathbf{r}) \cdot \mathbf{k}_F \sim 1/r$. Also knowing that $M(\omega)$ vanishes due to the gap symmetry, we can readily extract the field dependence of the $1/T_1$ for the d-wave state from Eq.(2) as

$$\frac{1}{T_1}(T \rightarrow 0, H) \sim \int_{\xi}^{R_H} dr^2 \left(\frac{1}{r}\right)^2 / \pi R_H^2 \sim H \log H, \quad (4)$$

and similarly for Knight shift as

$$K(T \rightarrow 0, H) \sim \int_{\xi}^{R_H} dr^2 \left(\frac{1}{r}\right) / \pi R_H^2 \sim \sqrt{H}. \quad (5)$$

In the case of the \pm s-wave state with small gap Δ_S and large gap Δ_L , again all we need to know is the DOS near zero energy in the mixed state. The author[3] has recently shown that the Doppler shifting energy $\mathbf{v}_s(\mathbf{r}) \cdot \mathbf{k}_F \sim \Delta_L/r$ overshoots the small gap to induce a constant DOS – which is basically the normal state DOS of the small gap band N_S^{norm} – around $\omega = 0$ in the small gap band in the region around the vortex core to the distance $r^* = \xi \frac{\Delta_L}{\Delta_S}$ that is a field independent constant. Hence the field dependencies of the NMR properties of the \pm s-wave state are the following.

$$\frac{1}{T_1}(T \rightarrow 0, H) \sim \int_{\xi}^{r^*} dr^2 (N_S^{norm})^2 / \pi R_H^2 \sim H \quad (6)$$

and

$$K(T \rightarrow 0, H) \sim \int_{\xi}^{r^*} dr^2 (N_S^{norm}) / \pi R_H^2 \sim H \quad (7)$$

where the contribution of $M(\omega)$ term is again neglected since its contribution is significant only near T_c and becomes negligible at low temperatures. The above field dependencies are for the ideally pure cases and we will show below, with numerical calculations, how these generic field dependencies are modified when the impurity scattering effect is included.

Numerical results and discussions.– We calculate the $1/T_1(T, H)$ and $K(T, H)$ including the impurity scattering effect using the SCTA[10, 11]. Once we calculate the impurity induced selfenergy – normal and anomalous – corrections, $\Sigma_{imp}^0(\omega, r)$ and $\Sigma_{imp}^1(\omega, r)$, respectively, we renormalize everywhere in the above formalism (Eqs. (1) -(3)) by $\tilde{\omega} = \omega + \Sigma_{imp}^0(\omega, r)$ and $\tilde{\Delta} = \Delta + \Sigma_{imp}^1(\omega, r)$ (Σ_{imp}^1 vanishes in the d-wave case due to the gap symmetry). In this paper, we considered only the strong coupling (unitary limit) non-magnetic impurity. The extension to the \pm s-wave state for the calculations of $N(\omega, r)$ and $M(\omega, r)$ with two bands is straightforward and referred to Ref.[3].

Figures 1 and 2 are the calculation results of the d-wave SC state. Fig. 1(a) shows the normalized $1/T_1(T)$ of the pure d-wave state with various field strengths. First, the zero field data displays an exact T^3 power law for all temperatures below T_c (for this we chose $2\Delta_0/T_c = 4$). Applying fields, the low temperature behavior immediately changes to the T -linear power indicating that the zero energy DOS is created by the magnetic field. Increasing the field strength, the magnitude of $1/T_1(T)$ at low temperatures progressively increases. In the inset, we plotted $1/T_1(T = 0.05T_c)$ vs H/H_c . As predicted in Eq.(4), the numerical data points (red circles) are perfectly fitted with $H \log H$ curve (black solid line; the fitting function is given in the inset with $h = H/H_{c2}$).

Figure 1(b) shows the same calculations as in Fig.1(a) but with impurity scattering. We chose the impurity concentration parameter $\Gamma = n_{imp}/\pi N_{tot}(0) = 0.03\Delta_0$ of the non-magnetic unitary scatterers. At zero field (black squares), $1/T_1(T)$ shows the typical T -linear at low temperatures due to the resonant (zero energy) impurity band but maintains the T^3 power law at higher temperatures. Applying fields, the overall line shape doesn't change but only the low temperature T -linear part progressively moves upward. It is clear that the zero energy DOS induced by the impurity scattering is additive to the field induced zero energy DOS by the Volovik effect. This result was not *a priori* expected because we calculated the position dependent impurity self-energy $\Sigma_{imp}^0(\omega, r)$ treating the Volovik effect and the impurity scattering on equal footing before we take the areal average. The plot of $1/T_1(T = 0.05T_c)$ vs H/H_c in the inset starts with a finite intercept at zero field, but still the data points are well fitted with $aH \log H + const.$ (black solid line).

Figure 2 is the calculation results of the normalized Knight shift $K(T)$ in parallel with the $1/T_1(T)$ in Fig.1. It reflects

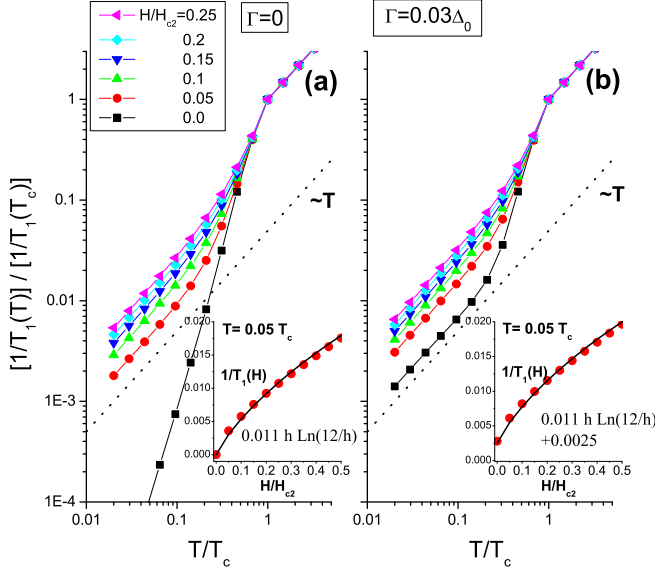


FIG. 1: (Color online) Normalized spin-lattice relaxation rates $[1/T_1(T)]/[1/T_1(T_c)]$ of the d-wave SC state with $2\Delta_0/T_c = 4$ for various magnetic field strengths, $H/H_{c2} = 0.0, 0.05, 0.1, 0.15, 0.2$ and 0.25 , respectively. (a) The results without impurities ($\Gamma = 0$). (b) The results with the impurity concentration $\Gamma = 0.03\Delta_0$ of the unitary scatterer. Insets of each panel are the $1/T_1$ vs H/H_{c2} at a fixed low temperature $T = 0.05T_c$.

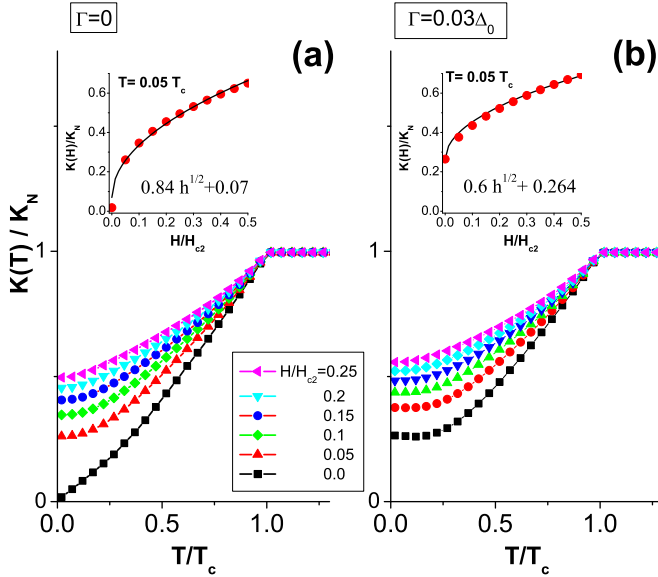


FIG. 2: (Color online) Normalized Knight shift $K(T)/K(T_c)$ of the d-wave SC state for various magnetic fields strengths, $H/H_{c2} = 0.0, 0.05, 0.1, 0.15, 0.2$ and 0.25 , respectively. (a) The results without impurities ($\Gamma = 0$). (b) The results with the impurity concentration $\Gamma = 0.03\Delta_0$ of the unitary scatterer. Insets of each panel are the $K(H)/K_N$ vs H/H_{c2} at a fixed low temperature $T = 0.05T_c$.

the same evolution of the DOS $\bar{N}(\omega, H)$ of the d-wave state with magnetic fields and impurities, as explained in Fig.1, onto $K(T)$. Fig.2(a) shows the normalized Knight shift $K(T)$ of the pure d-wave gap with various field strengths. First, the zero field data displays the T -linear power law at low temperatures as expected for the nodal gap. Applying fields, the low temperature part immediately becomes flat because of the field induced zero energy DOS and progressively moves upward with increasing the field strength. The inset shows $K(T = 0.05T_c)$ vs H/H_{c2} data and well fitted by the \sqrt{H} curve (black solid line) as shown in Eq.(5). Fig.2(b) shows the same calculations of $K(T)$ with impurity scattering as in Fig.1(b). The overall behavior and evolution of it are now easily understood with the additive zero energy DOSs induced by impurities and by the magnetic field. The plot of $K(T = 0.05T_c)$ vs H/H_{c2} data in the inset is well fitted by the $a\sqrt{H} + const.$ curve [12].

Figures 3 and 4 are the calculation results of $1/T_1$ and K of the $\pm s$ -wave SC state. We assumed two gaps with different sizes, $\Delta_S/\Delta_L = 0.4$. Other parameters are: (1) A rather large value of $2\Delta_L/T_c = 10$ was chosen to produce the much steep drop of $1/T_1(T)$ below T_c ; (2) $N_L(0)/N_S(0) = 2$ is freely chosen although there is a correlation between two ratios, Δ_S/Δ_L and $N_L(0)/N_S(0)$ [9]. As in the case of d-wave calculations, we considered only the unitary scatterers and assumed an equal strength between the interband and intraband scattering channels [11].

Figure 3(a) shows the normalized $1/T_1(T)$ of the pure $\pm s$ -wave state for various field strengths. First, the zero field $1/T_1(T)$ (black squares) displays the exponential drop for all temperature range without the coherence peak. The initial drop can be fitted by the T^6 power, much steeper –due to the choice of $2\Delta_L/T_c = 10$ – than the T^3 power that was often observed with many of Fe pnictide SC compounds. Applying fields, the low temperature behavior immediately changes to the quasi T -linear because of the zero energy DOS induced by the vortices as in the case of the d-wave gap. Increasing the field strength, the magnitude of $1/T_1(T)$ at low temperatures progressively increases. In the inset, we plotted $1/T_1(T = 0.05T_c)$ vs H/H_{c2} and the numerical data points (red circles) are perfectly fitted with the H -linear line (black dotted line) before it saturates when the small gap band becomes completely collapsed beyond the critical field strength $H^*/H_{c2} \sim (\Delta_S/\Delta_L)^2$ as predicted in Ref.[3].

Figure 3(b) shows the same calculations of $1/T_1(T)$ but with impurity scattering. The value of the impurity concentration $\Gamma = 0.08\Delta_L$ was slightly larger than the critical concentration of the $\pm s$ -wave model [11] ($\Gamma^* \approx 0.045\Delta_L$ in this case), which would produce a perfect V-shape DOS and hence the T^3 power law at low temperatures. Therefore, in our case, the zero field data of $1/T_1(T)$ (black squares) shows some power law in between T^3 and T -linear at low temperatures due to the combination of the finite zero energy DOS plus the V-shape DOS. Applying fields, the low temperature behavior immediately changes to the quasi T -linear as in the pure case of Fig.3(a) and the overall magnitude progres-

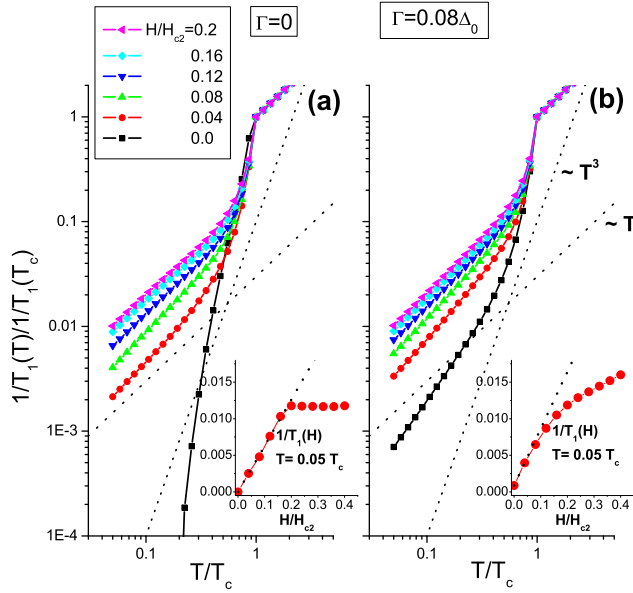


FIG. 3: (Color online) Normalized spin-lattice relaxation rates $[1/T_1(T)/1/T_1(T_c)]$ of the $\pm s$ -wave SC state for various magnetic fields $H/H_{c2} = 0.0, 0.04, 0.08, 0.12, 0.16$ and 0.2 , respectively. (a) The results without impurities ($\Gamma = 0$). (b) The results with the impurity concentration $\Gamma = 0.08\Delta_L$ of the unitary scatterer. Insets of each panel are the $1/T_1$ vs H/H_{c2} at a fixed low temperature $T = 0.05T_c$. Other parameters: $2\Delta_L/T_c = 10$, $\Delta_S/\Delta_L = 0.4$.

sively increases with increasing the field strength. The plot of $1/T_1(T = 0.05T_c)$ vs H/H_c in the inset of Fig.3(b) is much smoothed and there is no sharp kink at the saturation field $H^* \approx 0.16H_{c2}$; but the H -linear behavior still survives in the reduced region of low fields.

Figure 4 is the calculation results of the normalized Knight shift $K(T)$ of the $\pm s$ -wave SC state. Fig.4(a) shows the $K(T)$ of the pure $\pm s$ -wave gap with various field strengths. First, the zero field data displays the exponentially flat behavior at low temperatures reflecting the full gap superconductor. Applying fields, the low temperature part moves upward and also develops a T -linear part up to $H/H_{c2} \approx 0.12$. This behavior of $K(T) \sim a + bT$ at low temperatures is the result of the combination of the finite zero energy DOS plus the V-shape DOS – this is the typical feature of the multi-band $\pm s$ -wave SC state with the resonant impurity scattering[11] but it is now generated by the magnetic fields. The inset shows $K(T = 0.05T_c)$ vs H/H_c data which is well fitted by the H -linear line (black dotted line) as shown in Eq.(7) at low fields.

Figure 4(b) shows the same calculations of $K(T)$ including impurity scattering of $\Gamma = 0.08\Delta_L$. The overall behavior and evolution of it are again easily understood with the addition of the impurity induced DOS and the magnetic field induced DOS. The inset plot of $K(T = 0.05T_c)$ vs H/H_c data is much rounded and no kink feature is visible as in the inset of Fig.3(b). In general, all data of $K(T)$ calculations in Fig.2 and Fig.4 faithfully reflect the evolution of the total DOS $N_{tot}(\omega)$ at low frequencies by magnetic fields and im-

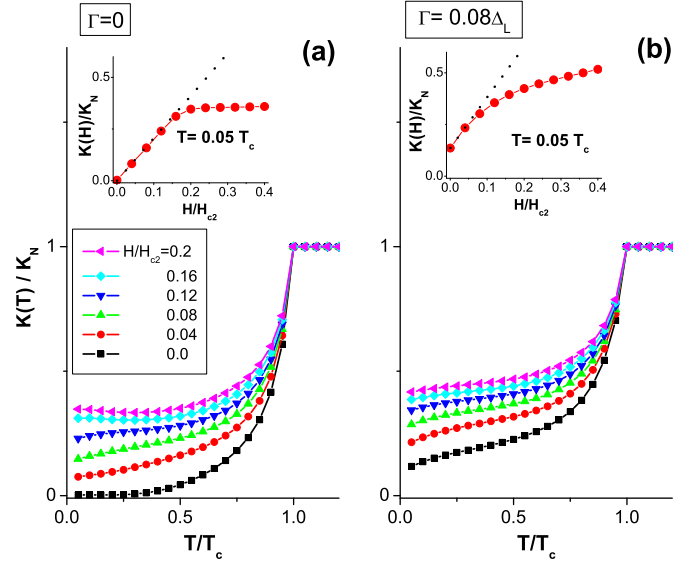


FIG. 4: (Color online) Normalized Knight shift $K(T)/K(T_c)$ of the $\pm s$ -wave SC state for various magnetic fields $H/H_{c2} = 0.0, 0.04, 0.08, 0.12, 0.16$ and 0.2 , respectively. (a) The results without impurities ($\Gamma = 0$). (b) The results with the impurity concentration $\Gamma = 0.08\Delta_L$ of the unitary scatterer. Insets of each panel are the $K(H)/K_N$ vs H/H_{c2} at a fixed low temperature $T = 0.05T_c$.

purity scattering as can be seen from Eq.(3).

Conclusion. – In summary, we extended the study of the Volovik effect on the NMR properties both in the d-wave and $\pm s$ -wave gap states. We derived the generic power laws of the field dependencies of $1/T_1(T \rightarrow 0, H)$ and $K(T \rightarrow 0, H)$ in pure cases. We also numerically calculated the full temperature dependencies of $1/T_1(T, H)$ and $K(T, H)$ for various field strengths, for both SC states, including impurity scattering. Main findings are: (1) the field dependence power laws of $1/T_1(T \rightarrow 0, H)$ and $K(T \rightarrow 0, H)$ are practically unchanged with impurity scattering in the d-wave case except for a constant shifting[12]. In the $\pm s$ -wave case, while the changes of the overall field dependencies are more significant, the generic power laws survive in a good part of low field region; (2) the Volovik effect acts as an equivalent pair breaker as the unitary impurity scatterers to creates the zero energy DOS and hence to modify the low temperature power laws of $1/T_1(T)$ and $K(T)$. It implies that the Volovik effect always needs to be taken into account for the analysis of the NMR experiments.

Acknowledgement – The author are grateful to Professor W. P. Halperin for showing us their data prior to publication and intensive discussions which directly motivated this work. We also acknowledge the discussions with G.Q. Zheng. The author (Y.B.) was supported by the Grant No. NRF-2010-0009523 and NRF-2011-0017079 funded by the National Research Foundation of Korea.

* ykbang@chonnam.ac.kr

- [1] G. E. Volovik, JETP Lett. **58**, 469 (1993).
- [2] C. Kubert and P.J. Hirschfeld, Solid State Commun. **105**, 459 (1998).
- [3] Y. Bang, Phys. Rev. Lett. **104**, 217001 (2010).
- [4] S. Oh, A. M. Mounce, W. P. Halperin, C. L. Zhang, P. Dai, A. P. Reyes, P. L. Kuhns, arXiv:1109.3834 (unpublished).
- [5] Y. Nakai, T. Iye, S. Kitagawa, K. Ishida, S. Kasahara, T. Shibauchi, Y. Matsuda, and T. Terashima, Phys. Rev. B **81**, 020503 (2010).
- [6] S. Kawasaki, C. Lin, P. L. Kuhns, A. P. Reyes, and Guo-qing Zheng, Phys. Rev. Lett. **105**, 137002 (2010); Guo-qing Zheng, H. Ozaki, Y. Kitaoka, P. Kuhns, A. P. Reyes, and W. G. Moulton, Phys. Rev. Lett. **88**, 077003 (2001).
- [7] I. Vekhter, P. J. Hirschfeld, and E. J. Nicol, Phys. Rev. B, **64**, 064513 (2001).
- [8] I.I. Mazin, D.J. Singh, M.D. Johannes, M.H. Du, Phys. Rev. Lett. **101**, 057003 (2008); K. Kuroki, S. Onari, R. Arita, H. Usui, Y. Tanaka, H. Kontani, and H. Aoki, Phys. Rev. Lett. **101**, 087004 (2008).
- [9] Y. Bang and H.-Y. Choi, Phys. Rev. B, **78**, 134523 (2008).
- [10] P. J. Hirschfeld, P. Wolfle, and D. Einzel, Phys. Rev. B **37**, 83 (1988); A. V. Balatsky, I. Vekhter, and J.-X. Zhu, Rev. Mod. Phys. **78**, 373 (2006).
- [11] Y. Bang, H.-Y. Choi, and H. Won, Phys. Rev. B **79**, 054529 (2009).
- [12] The dirty limit region where \sqrt{H} behavior is replaced by the $H \ln H$ form is restricted to the very low field region, $H/H_{c2} \ll 0.36 \Gamma/\Delta_0$ [2], which is $H/H_{c2} \ll 0.01$ in our calculations with $\Gamma/\Delta_0 = 0.03$.